Article

# 6-Hydroxyquinoline-*N*-oxides: A New Class of "Super" Photoacids

Kyril M. Solntsev, Caroline E. Clower, Laren M. Tolbert, and Dan Huppert

*J. Am. Chem. Soc.*, **2005**, 127 (23), 8534-8544• DOI: 10.1021/ja0514545 • Publication Date (Web): 21 May 2005



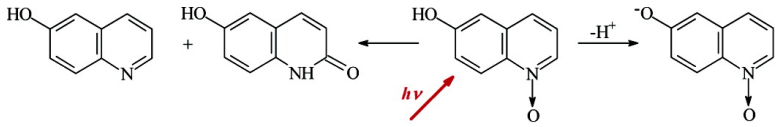


## More About This Article

Additional resources and features associated with this article are available within the HTML version:

- Supporting Information
- Links to the 5 articles that cite this article, as of the time of this article download
- Access to high resolution figures
- Links to articles and content related to this article
- Copyright permission to reproduce figures and/or text from this article

View the Full Text HTML

J|A|C|S
ARTICLES
Published on Web 05/21/2005

# 6-Hydroxyquinoline-*N*-oxides: A New Class of "Super" Photoacids[1]

Kyril M. Solntsev,*,† Caroline E. Clower,†,§ Laren M. Tolbert,*,† and Dan Huppert‡

*Contribution from the School of Chemistry and Biochemistry, Georgia Institute of Technology, Atlanta, Georgia 30332-0400, and Raymond and Beverly Sackler Faculty of Exact Sciences, School of Chemistry, Tel Aviv University, Tel Aviv 69978, Israel*

Received March 7, 2005; E-mail: solntsev@chemistry.gatech.edu; tolbert@chemistry.gatech.edu

***Abstract:*** N-Oxidation of hydroxyquinolines leads to a dramatic increase in their excited-state acidity. Time-resolved and steady-state emission characterization of 6-hydroxyquinoline-*N*-oxide and 2-methyl-6-hydroxyquinoline-*N*-oxide reveals a rich but less complex proton-transfer behavior than that of its parent hydroxyquinoline. The electronic effect of the oxidized heterocyclic nitrogen atom makes the excited state both less basic and more acidic than the parent and adds hydroxyquinoline *N*-oxides to the class of high-acidity excited-state proton donors in photochemistry and photobiology. Adiabatic photoinduced proton transfer is accompanied by the efficient nonreversible deoxygenation and 1−2 oxygen migration.

## 1. Introduction

The electron density in the excited state of naphthols is polarized toward the distal ring. Substitution on this ring by electron-withdrawing groups enhances the excited-state acidity.[2] Naphthols substituted at the 5- or 8-positions are especially photoacidic since the Hückel coefficients at these positions are larger in the excited state than in the ground state. Such photoacids have become particularly useful for fundamental time-resolved studies in excited-state proton transfer (ESPT).[3]

If, instead of substitution, replacement of C-5 or C-8 by nitrogen occurs to produce a hydroxyquinoline, similar electronic effects should occur. In addition, the enhanced electron density at nitrogen in the excited should make protonation at nitrogen a facile excited-state pathway. Indeed, such prototropic behavior has made the hydroxyquinolines a rich source of complex photodynamic studies.

**1.1. Background.** Excited-state proton transfer (ESPT) reactions have been extensively studied in bifunctional aromatic molecules possessing both proton-donating and -accepting groups. With such molecules, proton transfer can occur through H-bonded vicinal groups,[4−8] doubly H-bonded dimers,[9−12] a bridge of solvent molecules,[13−17] or intermolecular double proton transfer,[18,19] depending on the structure. 7-Hydroxy- (**7HQ**) and 8-hydroxyquinoline (**8HQ**) are compelling candidates for intramolecular excited-state proton transfer (ESPT). In *cis*-**7HQ** the photoinduced proton transfer from the hydroxyl group to the heterocyclic nitrogen can be facilitated by the chains of water,[20] alcohol,[21] ammonia,[22] and acetic acid[23] or by a polymer matrix.[24] In **8HQ** the intrinsic ground-state intramolecular hydrogen-bond leads to ultrafast intramolecular proton transfer in most solvents. For both **7HQ** and **8HQ** the excited-state phenomena involve multiple proton transfer coupled with a formal intramolecular electron transfer, so that the final ESPT products are ketonic tautomers rather than zwitterions.

In 6-hydroxyquinoline (**6HQ**) the distance between the proton-accepting and -donating functionalities is critically large

† Georgia Institute of Technology.
‡ Tel Aviv University.
§ Current address: Department of Natural Sciences, Clayton College & State University, Morrow, GA, 30260.

(1) This is part of our series "Photochemistry of "Super" Photoacids". For the previous paper see: Solntsev, K. M.; Sullivan, E. N.; Tolbert, L. M.; Ashkenazi, S.; Leiderman, P.; Huppert, D. *J. Am. Chem. Soc.* **2004**, *128*, 12701−12708.
(2) Agmon, N.; Rettig, W.; Groth, C. *J. Am. Chem. Soc*. **2002**, *124*, 1089−1096.
(3) Tolbert, L. M.; Solntsev, K. M. *Acc. Chem. Res*. **2002**, *35*, 19−27.
(4) Formosinho, S. J.; Arnaut, L. G. *J. Photochem. Photobiol. A* **1993**, *75*, 21−48.
(5) Kasha, M. *J. Chem. Soc., Faraday Trans. 2* **1986**, *82*, 2379−2392.
(6) Ormson, S. M.; Brown, R. G. *Prog. React. Kinet*. **1994**, *19*, 45−91.
(7) Ameer-Beg, S.; Ormson, S. M.; Brown, R. G.; Matousek, P.; Towrie, M.; Nibbering, E. T. J.; Foggi, P.; Neuwahl, F. V. R. *J. Phys. Chem. A* **2001**, *105*, 3709−3718.
(8) Douhal, A.; Lahmani, F.; Zewail, A. *Chem. Phys*. **1996**, *207*, 477−498.
(9) Hetherington, W. M., III; Micheels, R. H.; Eisenthal, K. B. *Chem. Phys. Lett.* **1979**, *66*, 230−233.
(10) Takeuchi, S.; Tahara, T. *J. Phys. Chem. A* **1998**, *102*, 7740−7753.
(11) Chou, P.; Yu, W.; Chen, Y.; Wei, C.; Martinez, S. S. *J. Am. Chem. Soc.* **1998**, *120*, 12927−12934.
(12) Folmer, D. E.; Wisniewski, E. S.; Castleman, A. W. *Chem. Phys. Lett.* **2000**, *318*, 637−643.
(13) Herbich, J.; Hung, C.; Thummel, R. P.; Waluk, J. *J. Am. Chem. Soc.* **1996**, *118*, 3508−3518.
(14) Mente, S.; Maroncelli, M. *J. Phys. Chem. A* **1998**, *102*, 3860−3876.
(15) Waluk, J. *Acc. Chem. Res*. **2003**, *36*, 832−838.
(16) Itoh, M.; Adachi, T.; Tokumura, K. *J. Am. Chem. Soc.* **1984**, *106*, 850−855.
(17) Konijnenberg, J.; Ekelmans, G. B.; Huizer, A. H.; Varma, C. A. *J. Chem. Soc., Faraday Trans. 2* **1989**, *85*, 39−51.
(18) (a) Lee, S. I.; Jang, D. J. *J. Phys. Chem.* **1995**, *99*, 7537−7541. (b) Kim, T. G.; Lee, S. I.; Jang, D. J.; Kim, Y. *J. Phys. Chem.* **1995**, *99*, 12698−12700.
(19) Bardez, E.; Boutin, P.; Valeur, B. *Chem. Phys. Lett.* **1992**, *191*, 142−148.
(20) (a) Fang, W.-H. *J. Phys. Chem. A* **1999**, *103*, 5567−5573. (b) Bardez, E. *Isr. J. Chem.* **1999**, *39*, 319−332.
(21) (a) Kohtani, S.; Tagami, A.; Nakagaki, R. *Chem. Phys. Lett*. **2000**, *316*, 88−93. (b) Matsumoto, Y.; Ebata, T.; Mikami, N. *J. Phys. Chem. A* **2002**, *106*, 5591−5599.
(22) Bach, A.; Tanner, C.; Manca, C.; Frey, H.-M.; Leutwyler, S. *J. Chem. Phys.* **2003**, *119*, 5933−5942.
(23) Chou, P.-T.; Wei, C.-Y.; Wang, C.-R. C.; Hung, F.-T.; Chang, C.-P. *J. Phys. Chem. A* **1999**, *103*, 1939−1949.
(24) Kwon, O.-H.; Doo, H.; Lee, Y.-S.; Jang, D.-J. *ChemPhysChem* **2003**, *4*, 1079−1083.


**10.1021/ja0514545 CCC: $30.25** 

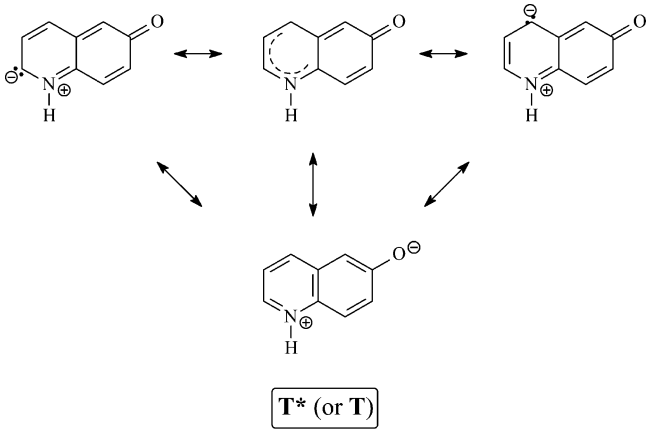


***Figure 1.*** Resonance hybrid structure of the tautomer of **6HQ** (ref 25). This is a zwitterions only in a formal sense, reflecting the formal charges in the most appropriate Lewis structure.

and no *direct* intramolecular proton transfer (even through solvent chains) has been observed. Nevertheless, by analogy to *trans*-**7HQ** in neutral water, the ESPT mechanism in **6HQ** involves ultrafast dissociation resulting in an excited-state anion, which in turn, as a "super"photobase, abstracts proton from the solvent, forming a zwitterion.[25] At a pH low enough to protonate nitrogen ($<pK_a = 5.1$) **6HQ** exists as a cation in the ground state. After excitation it also undergoes ultrafast deprotonation resulting in the same tautomer as that at neutral pH. In basic solutions at pH greater than that for hydroxyl group deprotonation ($>pK_a = 9.1$), the anion undergoes protonation in the excited state, again resulting in the tautomer. Excited-state deprotonation of the hydroxyl group is effective even in 10 M perchloric acid solutions, and protonation of the nitrogen occurs in 12 M sodium hydroxide![25] In all cases there is no evidence of back-reaction, i.e., reprotonation of the naphtholate. All of these phenomena are the result of coupled proton and electron transfers in the excited state (tautomerization), which result in the formation of the zwitterion **6HQ(T)*** shown in Figure 1. Unfortunately, emission from **6HQ(T)*** is very weak, thus limiting the applications of the molecule as a fluorescent probe.[20b,26]

The photoacidity of hydroxyquinoline compounds can be further perturbed by increasing the electronegativity of the heterocyclic ring. It has been shown that the electron-withdrawing effect of the quarternated nitrogen, achieved by methylation of the heterocyclic nitrogen, is significant enough to increase the acidity of the hydroxyl group and thus lower the ground-state $pK_a$ by 2 units.[25a] This is similar to the effects observed for naphthol compounds substituted on the distal ring with electron-withdrawing groups.[3] A recent time-resolved study on photoinduced proton transfer from *N*-methyl-6-hydroxyquinolinium[27] demonstrated a remarkable photoacidity of this compound: protolytic photodissociation in water occurs at 2 ps. This rate for intermolecular ESPT to water is among the fastest reported to date. An alternative approach, which avoids creating an organic salt, is to modify the acidity of **6HQ** by converting the latter into 6-hydroxyquinoline-*N*-oxide, preserving the electronegativity of the molecule.

Aromatic *N*-oxides, including quinoline *N*-oxides,[28] are a well-studied group of compounds. The spectroscopy and mechanistic photochemistry of many aromatic *N*-oxides, and quinoline *N*-oxides in particular (but not hydroxyquinoline *N*-oxides), has been studied in detail.[29] Absorbance spectra of quinoline *N*-oxides have complex structures that include mixing of $\pi-\pi^*$ and $n-p^*$ transitions.[28−30] The latter undergo well-documented hypsochromic shifts with the increase of solvent polarity. Two major photoconversion processes have been documented for aromatic *N*-oxides: deoxygenation and intermediate oxaziridine formation followed by rearrangement. Such enhanced photo-, as well as thermal reactivity of *N*-oxides has been utilized in biology, resulting in their application as antitumor agents[31] (such as tripazamine[32]) and as herbicidal agents.[33] Some naturally occurring aromatic *N*-oxides, including metabolic products, are known to be strong toxins.[34] It is worth noting that an alkyl-substituted hydroxyquinoline-*N*-oxide, 2-*n*-heptyl-4-hydroxyquinoline-*N*-oxide (HQNO), is a widely used effective respiratory-chain inhibitor.[35] Its fluorescence in water[36] at pH 7.5 exhibits a large Stokes shift of 7300 $cm^{-1}$, which may be an indication for efficient ESPT.

A very popular dye indicator Alamar Blue (resazurin, 7-hydroxy-3H-phenoxazin-3-one *N*-oxide) is another common hydroxyaromatic *N*-oxide. The "resazurin reduction test" has been used for about 50 years to monitor bacterial and yeast contamination of milk, and also for assessing semen quality. Today it is used to monitor cytotoxic activity and cell proliferation of a wide array of biological samples. A pronounced color change ultimately leading to decoloration of resazurin caused by the N−O group deoxygenation is explained by the reaction of the dye with the reducing substances during bacterial metabolism.[37] It is interesting that only the reduced form of resazurin is fluorescent and can be used for cell imaging.[38]

(25) (a) Bardez, E.; Chatelain, A.; Larrey, B.; Valeur, B. *J. Phys. Chem.* **1994**, *98*, 2357−2366. (b) Kim, T. G.; Kim, Y.; Jang, D.-J. *J. Phys. Chem. A* **2001**, *105*, 4328−4332. (c) Poizat, O.; Bardez, E.; Buntinx, G.; Alain, V. *J. Phys. Chem. A* **2004**, *108*, 1873−1880.
(26) Bardez, E.; Fedorov, A.; Berberan-Santos, M. N.; Martinho, J. M. G. *J. Phys. Chem. A* **1999**, *103*, 4131−4136.
(27) Kim, T. G.; Topp, M. R. *J. Phys. Chem. A* **2004**, *108*, 10060−10065.
(28) Jones, G.; Baty, D. J. In *Quinolines. Part II*; Jones, G., Ed.; Wiley: Chichester, 1982; Chapter 3.
(29) Reviews: (a) Spence, G. G.; Taylor, E. C.; Buchardt, O. *Chem. Rev.* **1970**, *70*, 231−265. (b) Bellamy, F.; Streith, J. *Heterocycles* **1976**, *4*, 1391−1447. (c) Albini, A.; Alpegiani, M. *Chem. Rev.* **1984**, *84*, 43−71. (d) Kurasawa, Y.; Takada, A.; Kim, H. S. *J. Heterocycl. Chem.* **1995**, *32*, 1085−1114.
(30) (a) Kubota, T.; Miyazaki, H. *Chem. Pharm. Bull.* **1961**, *9*, 948−961. (b) Andreev, V. P.; Ryzhakov, A. V. *Chem. Heterocycl. Cmpd.* **1993**, *29*, 1435−1440.
(31) (a) Wardman, P.; Dennis, M. F.; Everett, S. A.; Patel, K. B.; Stratford, M. R. L.; Tracy, M. *Biochem. Soc. Symp.* **1995**, *61*, 171−194. (b) Cerecetto, H.; González, M. *Mini-Rev. Med. Chem.* **2001**, *1*, 219−231.
(32) (a) Fuchs, T.; Gates, K. S.; Hwang, J.-T.; Greenberg, M. M. *Chem. Res. Toxicol.* **1999**, *12*, 1190−1194. (b) Ban, F.; Gauld, J. W.; Boyd, R. J. *J. Am. Chem. Soc.* **2001**, *123*, 7320−7325. (c) Inbaraj, J. J.; Motten, A. G.; Chignell, C. F. *Chem. Res. Toxicol.* **2003**, *16*, 164−170. (d) Birincioglu, M.; Jaruga, P.; Chowdhury, G.; Rodriguez, H.; Dizdaroglu, M.; Gates, K. S. *J. Am. Chem. Soc.* **2003**, *125*, 11607−11615. (e) Shi, X.; Platz.; M. S. *J. Phys. Chem. A* **2004**, *108*, 4385−4390.
(33) Cerecetto, H.; Dias, E.; Di Maio, R.; Gonzalez, M.; Pacce, S.; Saenz, P.; Seoane, G.; Suescun, L.; Mombru, A.; Fernandez, G.; Lema, M.; Villalba, J. *J. Agric. Food Chem.* **2000**, *48*, 2995−3002.
(34) (a) Williams, L.; Chou, M. W.; Yan, J.; Young, J. F.; Chan, P. C.; Doerge, D. R. *Toxicol. Appl. Pharm.* **2002**, *182*, 98−104. (b) Karlson-Stiber, C.; Persson, H. *Toxicon* **2003**, *42*, 339−349.
(35) (a) Rothery, R. A.; Weiner, J. H. *Eur. J. Biochem.* **1998**, *254*, 588−595. (b) Maklashina, E.; Cecchini, G. *Arch. Biochem. Biophys.* **1999**, *369*, 223−232. (c) Nakayama, Y.; Hayashi, M.; Yoshikawa, K.; Mochida, K.; Unemoto, T. *Biol. Pharm. Bull.* **1999**, *22*, 1064−1067. (d) Rothery, R. A.; Blasco, F.; Weiner, J. H. *Biochemistry*, **2001**, *40*, 5260−5268. (e) Simkovic, M.; Frerman, F. E. *Biochem. J.* **2004**, *378*, 633−640.
(36) Van Ark, G.; Berden, J. A. *Biochim. Biophys. Acta* **1977**, *459*, 119−137.
(37) (a) Thomas, S. B.; Jones, T. Idwal; Griffiths, D. G. *Dairy Ind.* **1963**, *28*, 812−17. (b) McMillian, M. K.; Li, L.; Parker, J. B.; Patel, L.; Zhong, Z.; Gunnett, J. W.; Powers, W. J.; Johnson, M. D. *Cell Biol. Toxicol.* **2002**, *18*, 157−173. (c) Hamid, R.; Rotshteyn, Y.; Rabadi, L.; Parikh, R.; Bullock, P. *Toxicol. in Vitro* **2004**, *18*, 703−710.

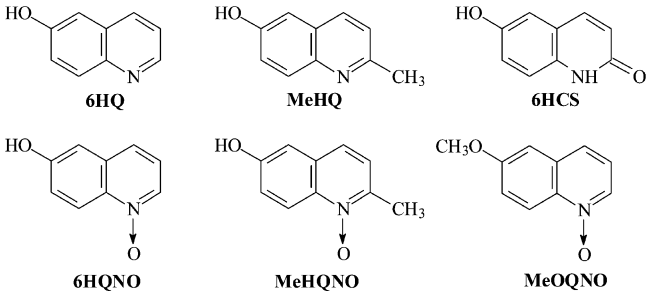


***Figure 2.*** Chemical structures of the investigated compounds.

The acid−base chemistry of quinoline *N*-oxides, in both the ground- and excited states, differs from that of the parent quinolines. In the ground state, the p$K_a$'s of the protonated quinoline *N*-oxides[39] are about 4 units lower than those of corresponding quinolinium ions. A more striking difference is observed in the excited state. While quinolines and their derivatives are known to act as photobases,[40] the basicity of *N*-oxides decreases by about 4 p$K_a$ units upon excitation.[39]

6-Hydroxyquinoline-*N*-oxide has been mentioned as a byproduct in the syntheses of antiplatelet agents,[41] novel chelates,[42] and antiviral agents.[43] No spectroscopic studies have been reported in these cases. We now report the effects of *N*-oxidation on the ground- and excited-state proton-transfer reactions of **6HQ** derivatives in which the overall charge of the molecule is not changed. 6-Hydroxyquinoline-*N*-oxide and 2-methyl-6-hydroxyquinoline-*N*-oxide have been synthesized and studied using absorption, steady-state fluorescence, and time-resolved fluorescence techniques. Irreversible photochemical transformations of these *N*-oxides have been also been investigated.

## 2. Experimental Section

6-Hydroxyquinoline (**6HQ**) and 6-methoxyquinoline-*N*-oxide (**MeOQNO**) were purchased from Aldrich. 2-Methyl-6-hydroxyquinoline (**MeHQ**) was purchased from Alfa Aesar. 6-Hydroxyquinoline-*N*-oxide (**6HQNO**) was synthesized by treatment of the **6HQ** with 3-chloroperoxybenzoic acid (MCPBA), purified, and characterized as previously described.[41] 2-Methyl-6-hydroxyquinoline-*N*-oxide (**MeHQNO**) was synthesized by the same method using the corresponding quinoline (see Figure 2 for structures).

The $^1$H and $^{13}$C NMR spectra were obtained on a Bruker DRX 500 spectrometer in DMSO-$d_6$ solution. Chemical shifts, in ppm, are referred to TMS. The FTIR spectra were taken in KBr matrix on a Nicolet 4700 spectrometer. Abbreviations: s = strong, vs = very strong. Mass spectra were taken in electron impact mode using a VG Instruments 70SE spectrometer.

Spectral data for **MeHQNO**:

$^{13}$C NMR 156.52; 141.80; 135.66; 130.61; 123.62; 122.75; 121.73; 120.49; 109.24; 17.85.

$^1$H NMR 10.3 (br, 1H); 8.40 (d, $J_{HH}$ = 9 Hz, 1H); 7.63 (d, $J_{HH}$ = 8.5 Hz, 1H); 7.44 (d, $J_{HH}$ = 8.5 Hz, 1H); 7.30 (dd, $J_{HH}$ = 9 Hz, 3.0 Hz, 1H); 7.20 (d, $J_{HH}$ = 3.0 Hz); 2.50 (s, 3H).

EIMS *m*/z(%) 175.1(86); 159.1(77); 158.1(100); 144(5.0); 130.0(17); 103.1(13); 81.1(10); 69.1(20).

FTIR (cm$^{-1}$) 3660−1950 (broad with local maxima at ca. 3448, 2960, and 2517); 1632; 1615; 1570(s); 1518; 1451; 1434; 1397; 1330(s); 1312(s); 1275; 1260; 1225(s); 1194; 1174(vs); 1136; 1092; 931; 879; 834; 809(s); 732; 655; 603; 591.

Spectroscopic measurements were carried out in methanol/water mixtures prepared by the volumetric method. The methanol solvent was BDH HPLC grade with <0.05% water. Deionized water (resistivity > 10 MΩ/cm) was used for dilutions. Solvents contained no detectable fluorescent impurities and were used without further purification. All experiments were performed at room temperature (ca. 22 °C). Steady-state fluorescence spectra of nondeoxygenated solutions were recorded on a SPEX spectrofluorometer and corrected using the method described previously. Transient fluorescence was detected using the time-correlated single-photon counting (TCSPC) method. A synchronized, cavity dumped picosecond Rhodamine 6G dye laser, driven by a Nd:YAG laser, was used as a source of excitation. The excitation wavelength in all time-resolved experiments was set to 310 nm. The time resolution varied from 4.88 to 97.7 ps/channel while the instrument response function (IRF) at the short time scales had a full-width at half-maximum of about 40 ps. TCSPC had limited time resolution of about 20 ps after deconvolution.[45]

Preparative irradiation was performed using a 450 W Hanovia mercury lamp with a Pyrex filter or using monochromated light of the fluorimeter lamp with the wide open excitation slits. Photochemical quantum yields were determined using the standard azobenzene actinometry method.[46] NMR spectra of the photolysis products were recorded on Varian Gemini series 300 MHz spectrometer.

## 3. Results

We have found that the spectral behavior of **6HQ** and its *N*-oxide changes very little upon 2-methylation, so most of the spectral data related to **MeHQ** and **MeHQNO** have been placed in the Supporting Information.

**3.1. Spectroscopic Measurements and pH Titrations. 6HQNO** is well-soluble in water, demonstrating good linearity in the Beer's Law plot ($\epsilon$ = 4275 M$^{-1}$ cm$^{-1}$ at 320 nm) up to 0.4 mM. However, other compounds, such as **MeHQ** tend to aggregate. Thus, the study of the pH dependence of emission and absorbance in methanol/water mixtures is required to avoid aggregation. In our previous paper we reported absorbance and emission properties of **6HQ** in a 1/1 v/v MeOH/$H_2O$ mixture[47] (MW) over a very wide pH range.[1] In this mixed solvent the dissociation constants for many phenols increase by 0.3−1.0 p$K_a$ unit as compared to that of bulk water, while dissociation constants of protonated amines decrease, but less significantly.[48]

The absorption spectra of *N*-oxides **6HQNO** and **MeHQNO** in methanol solution (Figure 3) and in MW at neutral pH (Figures 4 and S1[49]) differed strongly from those of the parent hydroxyquinolines. The low-energy absorbance bands of *N*-oxides in methanol consisted of a main peak at 323 nm for **6HQNO** and 317 nm for **MeHQNO** and a shoulder around 350 nm for both compounds. The methylated compound had a slight bathochromic shift in the hydroxyquinoline pair and a hypsochromic shift in the *N*-oxide pair (Figure 3). Solution pH measurements were performed in MW with a glass electrode

(38) (a) Reyes, R.; Martinez, J. C.; Delgado, N. M.; Merchant-Larios, H. *Arch. Androl*. **2002**, *48*, 209−219. (b) *Handbook of Fluorescent Probes and Research Products*, 9th ed.; Haughland, R. P.; Ed.; Molecular Probes: Eugene, OR, 2003; Chapter 15.2.
(39) (a) Favaro, G. *Mol. Photochem*. **1971**, *2*, 323−329. (b) Aloisi, G. G.; Favaro, G. *J. Chem. Soc., Perkin Trans. 2* **1976**, *4*, 456−460.
(40) Weller, A. *Prog. React. Kinet*. **1961**, *1*, 189−214.
(41) Wang, T.-C.; Chen, Y.-L.; Lee, K.-H.; Tzeng, C.-C. *Synthesis* **1997**, *1*, 87−90.
(42) Hoegberg, S.; Elman, B.; Liem, H.; Madan, K.; Moberg, C.; Muhammed, M.; Sjoeberg, B.; Weber, M. World Patent WO8401947, 1984.
(43) Wang, T.; Wallace, O. B.; Meanwell, N. A.; Kadow, J. F.; Zhang, Z.; Yang, Z. World Patent WO2003092695, 2003.
(44) Gardecki, J. A.; Maroncelli, M. *Appl. Spectrosc*. **1998**, *52*, 1179−1189.
(45) Genosar, L.; Cohen, B.; Huppert, D. *J. Phys. Chem. A* **2000**, *104*, 6689−6698.
(46) Gauglitz, G.; Hubig, S. *J. Photochem*. **1981**, *15*, 255−257.
(47) 0.692 molar fraction $H_2O$.
(48) Rosés, M.; Rived, F.; Bosch, E. *J. Chromatogr., A* **2000**, *867*, 45−56.
(49) See Supporting Information for more data, details, and analysis.

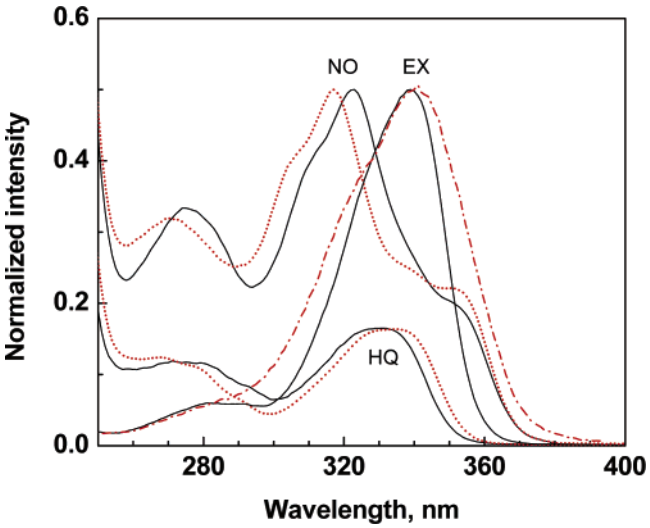


***Figure 3.*** Absorption spectra of **6HQ** (HQ solid line), **MeHQ** (HQ dotted line), **6HQNO** (NO solid line), **MeHQNO** (NO dotted line) in methanol. Excitation spectra of **MeHQ** (EX solid line) and **MeHQNO** (EX dash−dotted line) in methanol are also presented. Two latter spectra were monitored at 380 nm (see Figure 6).

precalibrated in aqueous buffer.[50] The absorption spectra of **MeHQ** in MW at all pH values were close to that of **6HQ** (Figures 4 and S1[49]) demonstrating transformation between cationic, neutral, and anionic species. Upon transition to mixed solvent, the dominating low-energy absorption peak of the *N*-oxides underwent a slight blue-shift, to 318 nm for **6HQNO** and to 315 nm for **MeHQNO**. With a pH decrease to 1.4 the shoulder seen at 350 nm in the neutral absorption clearly became a second peak. At low pH the absorption spectra of hydroxyquinolines and their *N*-oxides were identical. Similarly to the behavior of hydroxyquinolines, with a pH increase up to 10.6 in MW, a new low-energy band appeared in the *N*-oxide absorbance spectra with maxima at 385 nm for **6HQNO** and 382 nm for **MeHQNO**. The spectral transformation in the acidic region could be assigned to the protonation of the heterocyclic nitrogen for hydroquinolines[25a] and of the N−O group for *N*-oxides. High pH transitions were apparently due to hydroxyl group deprotonation. Only one acid−base transition associated with protonation of the N−O group was observed for **MeOQNO** (Figure S1).[49] The acid−base dissociation constants could be determined by monitoring the absorbance at 372 and 385 nm for the acidic and basic regions, respectively. The titration curves are presented in Figure 5. The acidity constants ($pK_a$) values calculated from the titration data are as given in Table 1.

**3.2. Emission Spectra.** *N*-Oxidation strongly influenced the emission properties of hydroxyquinolines, although the ground-state properties of hydroxyquinolines and their *N*-oxides were similar. For instance, unlike hydroxyquinolines[51] the *N*-oxides exhibited dual fluorescence spectra (Figure 6) even in bulk methanol, while **6HQ** and **MeHQ** showed no ESPT. We should note, however, that the emission of hydroxyquinolines in methanol was extremely sensitive to the presence of water and tiny amounts of the latter led to a small but detectable tautomer emission at 595 nm (Figure 6). No ESPT was observed for **6HQNO** in $Me_2SO$, although the emission maxima were shifted to 420 nm (data not shown). The excitation spectra of hydroxyquinolines in methanol monitored at the emission maxima matched the absorbance spectra well (Figure 3). However, the maxima of the excitation spectra of the *N*-oxides in methanol corresponded to a weak low-energy shoulder in the absorbance spectra of these compounds (Figure 3). With the addition of water we observed a substantial decrease in the fluorescence intensity of the high-energy band at 405 nm for **6HQNO** (380 nm for **Me6HQNO**) and a concomitant increase of the band at 530 nm (520 nm for **MeHQNO**). In MW solutions the high-energy peak almost disappeared (graph 5 at Figure 7 and graph 3 at Figure S2).[49]

The emission spectra of **6HQ** in MW solutions in the 1.8−12.3 pH range were discussed in our previous publication.[1] They resembled the spectral pH-dependence of **6HQ** in pure water analyzed in detail by Bardez et al.,[25a] who expanded the acidity range to solutions of very concentrated $HClO_4$ and NaOH. As was mentioned earlier, the emission spectrum of **6HQNO** in MW at neutral pH consisted mostly of an intense band at 525 nm (graph 5 at Figure 7) and a very weak high-energy shoulder at 405 nm with a small increase of the 420 nm band was observed.

With decreasing pH to 1.8 the strong quenching of the long-wavelength band concomitant with a small increase of the 420 nm band was observed. This was in contrast to **6HQ** behavior, where the dominating tautomer emission at 590 nm was practically pH-independent.[25a] A further pH decrease to 0 resulted in simultaneous quenching of both bands and their bathochromic shift to 550 and 435 nm, respectively. An inflection point in the titration curve was observed around pH 2.6 (Figure 5). Upon further acidification up to 5.5 M $HClO_4$ a dramatic increase of 445 nm emission band was observed (graph 4 at Figure 7), similar to **6HQ** (graph 1 at Figure 7).

With increasing pH the emission band of **6HQNO** at 405 nm totally converted into a long-wavelength emission at 525 nm (graph 6 at Figure 7). Under the same conditions the dominating emission of **6HQ** was from the tautomer. The emission of the neutral form converted into the anionic form due to ground-state deprotonation[25a] (graph 3 at Figure 7). Similar behavior was observed for **MeHQ**−**MeHQNO** pair at the whole pH range (Figure S2).[49]

**3.3. Photoproducts and Quantum Yields.** During extended fluorescence experiments, especially during time-resolved measurements with laser excitation, the emission of *N*-oxides changed in color from bright green into blue. Photolysis experiments of **6HQNO** and **MeHQNO** in different solvents demonstrated that excessive UV-irradiation led to irreversible decomposition of these compounds. The parent hydroxyquinolines underwent no irreversible photochemical transformation at these conditions. *N*-oxides were stable during storage in the dark at room temperature without air removal.

Irradiation of **6HQNO** and **MeHQNO** with Pyrex-filtered light from a Hanovia 450-W medium-pressure mercury lamp was performed in aerobic solutions at different time intervals. Oxygen was not removed to make direct comparison to a routine series of fluorescence steady-state and time-resoled measure-

(50) (a) Bosch, E.; Bou, P.; Allemann, H.; Rosés, M. *Anal. Chem.* **1996**, *68*, 3651−3657. (b) Avdeef, A.; Box, K. J.; Comer, J. E. A.; Gilges, M.; Hadley, M.; Hibbert, C.; Patterson, W.; Tam, K. Y. *J. Pharm. Biomed. Anal.* **1999**, *20*, 631−641. (c) Canals, I.; Portal, J. A.; Bosch, E.; Rosés, M. *Anal. Chem.* **2000**, *72*, 1802−1809. (d) Canals, I.; Valko, K.; Bosch, E.; Hill, A. P.; Rosés, M. *Anal. Chem.* **2001**, *73*, 4937−4945. (e) Canals, I.; Oumada, F. Z.; Rosés, M.; Bosch, E. *J. Chromatogr., A* **2001**, *911*, 191−202.

(51) Mehata, M. S.; Joshi, H. C.; Tripath, H. B. *Chem. Phys. Lett.* **2002**, *359*, 314−320.

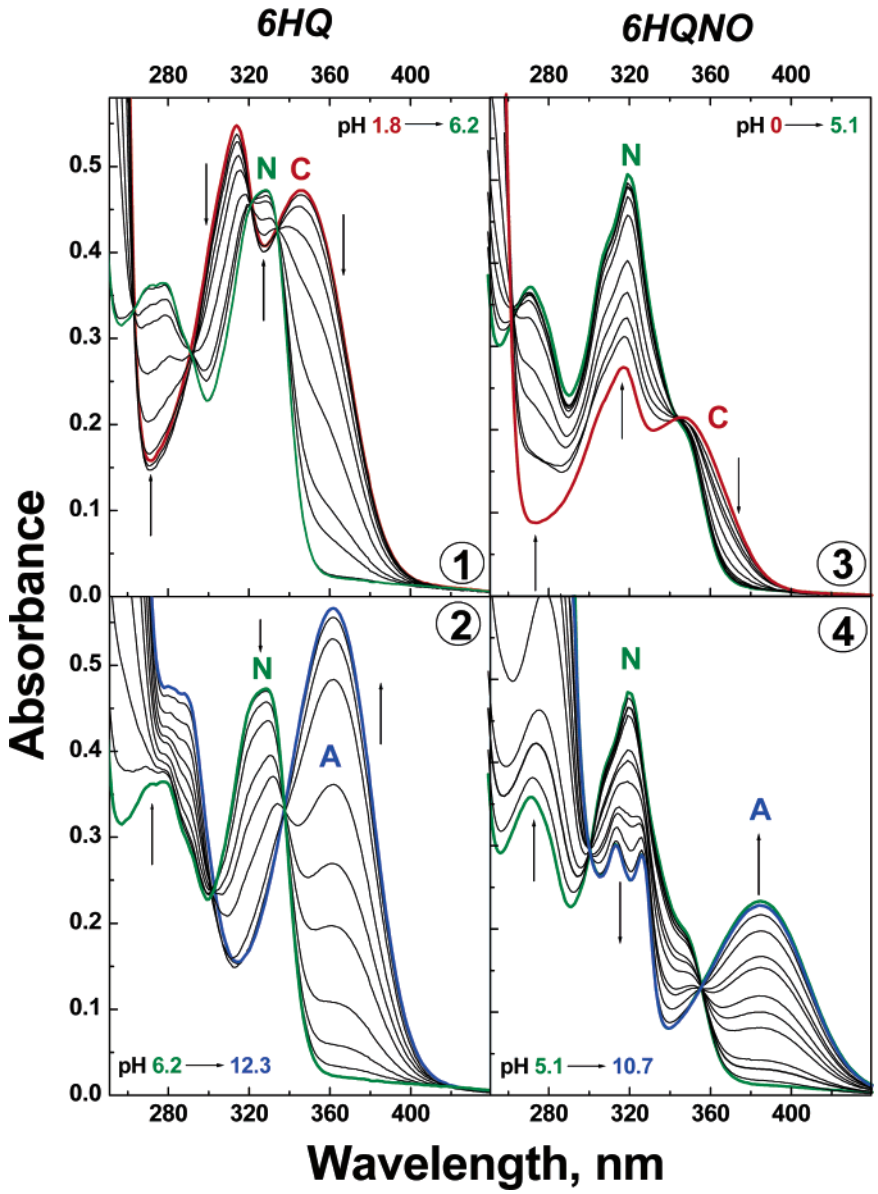


***Figure 4.*** The absorption spectra of **6HQ** and **6HQNO** in 1/1 v/v. water−methanol mixture as function of pH. (1) **6HQ** in acidic pH region; (2) **6HQ** in basic pH region; (3) **6HQNO** in acidic pH region; (4) **6HQNO** in basic pH region. Absorbance bands of neutral, cationic, and anionic species are marked as N, C, and A, respectively.

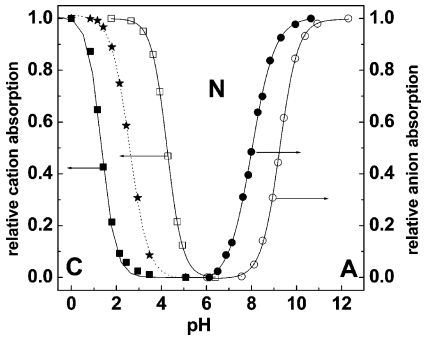


***Figure 5.*** Steady-state titrations curves of **6HQ** and **6HQNO** in 1/1 v/v water-methanol mixture. Open squares and open circles: absorbance data for **6HQ**; closed squares and closed circles: absorbance data for **6HQNO**; stars: inverse relative anionic emission of **6HQNO** at 520 nm. N, C, and A are the acidity areas of existence of neutral, cationic, and anionic species, respectively.

ments at various pHs. Alternatively, the photolysis was performed in the cuvette holder of the fluorimeter with the excitation slits wide open. The decomposition of *N*-oxides and the accumulation of photoproducts were monitored by NMR, absorbance, and fluorescence spectroscopy. A simple photochemical transformation was observed for **MeHQNO**. Upon irradiation in $CD_3OD$, this compound was converted quantitatively into parent **Me6HQ** (Figure 8a). The reaction was complete after 75 min. No other products were detected. Photolysis of **6HQNO** was more complicated. After 15 min of irradiation, 6-hydroxycarbostyril (6-hydroxyquinolin-2(1*H*)-one, **6HCS**)[41] formation, characterized by a doublet around 6.6 ppm, was observed (Figure 8b). A small fraction of the parent **6HQ**

***Table 1.*** Ground-State p$K_a$ in MW

| | $-N(O)H^+ \leftrightarrow -N(O) + H^+$ | $-OH \leftrightarrow -O^- + H^+$ |
|---|---|---|
| **6HQ**[1] | 4.25 | 9.25 |
| **MeHQ** | 5.01 | 9.68 |
| **6HQNO** | 1.32 | 8.01 |
| **MeHQNO** | 1.66 | 8.75 |
| **MeOQNO** | 1.00 | - |

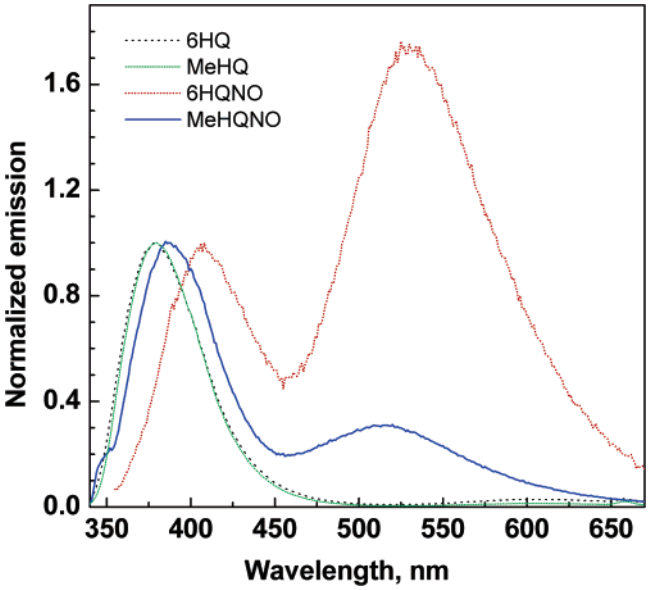


***Figure 6.*** Emission spectra of the investigated compounds in methanol. In all cases the excitation wavelengths were long-wavelength absorption maxima.

also formed. The photodecomposition rates for **MeHQNO** and **6HQNO** after 15 min irradiation were comparable (about 60%). After 75 min of photolysis the photolysis of **6HQNO** was complete. **6HCS** and **6HQ** were formed at a ratio of 3/2.

Several additional photolysis experiments were performed. Photodecomposition of **6HQNO** after 15 min irradiation in $D_2O$ was much less efficient than in $CD_3OD$. However irradiation for 75 min resulted in the same products as in $CD_3OD$: **6HCS** and **6HQ** (Figure S3).[49] The ratio of product yields differed from that of in $CD_3OD$, ca. 2:3. To check the hypothesis that deoxygenation of *N*-oxides involved hydrogen atom abstraction, we performed photolysis of **MeHQNO** in *t*-BuOH, a much weaker H atom donor than methanol.[52] As in the case of $CD_3OD$, we observed only one photochemical product: the parent **MeHQ** (Figure S4).[49] However, the relative yield of **MeHQ** after 75 min photolysis in *t*-BuOH[49] was about the same as that after 30 min photolysis in $CD_3OD$ (see Figure 8b) demonstrating much slower photodecomposition in *t*-BuOH.

To check whether efficiency of photolysis was associated with ESPT, **MeOQNO** was irradiated under the same conditions as the other *N*-oxides.[49] A 15 min photolysis of **MeOQNO** in $CD_3OD$ resulted in the formation of 6-methoxycarbostyril with a yield comparable to those of other photoproducts of **6HQNO** and **MeHQNO** (Figures S5 and S6).[49] An irradiation at longer times resulted in the formation of an unidentified product, perhaps the result of ring contraction. No 6-methoxyquinoline was formed.

The photolysis of the *N*-oxides was also monitored and quantified using UV-spectroscopy. As an example we demonstrate a conversion of the **MeHQNO** absorption spectrum into the spectrum of parent **MeHQ** (Figure 9) in the course of photolysis in MW. Quantum yields for the decomposition of **6HQNO** and **MeHQNO** in MeOH and MW were determined spectrophotometrically at low conversion ($\lambda_{exc} = 337$ nm, $\lambda_{obs}$ = low-energy maxima for each compound) using azobenzene actinometry and were found compound- and solvent-independent ($\phi = 0.054 \pm 0.002$). The quantum yield of **MeOQNO** decomposition in methanol was about 2.5 times larger.

**3.4. Time-Resolved Measurements.** As was demonstrated in the previous section all *N*-oxides underwent effective photodecomposition under extended illumination. This effect was especially visible in the time-resolved measurements. However, our knowledge of the photodecomposition products and efficiency made possible a separation of fluorescence kinetic signals from starting *N*-oxides and products of photolysis. The simplest case was obviously **MeHQNO**, which underwent only simple deoxygenation. The fluorescence decay of **MeHQNO** monitored at 380 nm was clearly bimodal (curve A in Figure 10). Biexponential deconvolution fit with a $\chi^2 = 1.06$ resulted in a dominating fast decay component with a lifetime of ca. 250 ps and a slower component with a lifetime of 2.2 ns. Depending on the exposure time, the age of the solution, and the use of the cell with internal stirring, the relative amplitude of the longest component varied over a wide range, while the lifetimes of both components remained the same. The fluorescence decay of the parent **MeHQ**, which could not undergo ESPT in methanol (monitored at 380 nm), had a lifetime of 2.2 ns (curve C in Figure 10). Taking into account our knowledge of the photolysis mechanism, we related the longest component in **MeHQNO** decay to the product of decomposition—the parent **Me6HQ**—and the fastest component to the decay of **MeHQNO** undergoing ESPT. The three-exponential fit with a $\chi^2 = 1.06$ of the fluorescence time-resolved signal of **MeHQNO** monitored at 560 nm (curve B in Figure 10) has a 240 ps rise component and 1.29 ns and 9.4 ns decay components. The module amplitude of the rising components was more than 4 times smaller that the sum of the decaying components amplitudes. The decay of **MeHQNO** in basic methanol solution had a lifetime 11.0 ns (curve D in Figure 10). With the addition of water to methanol solution of **MeHQNO** the lifetime of the short component in 380 nm decreased significantly and reached 38 ps in MW (Figure S7).[49]

Similar but more complex kinetic behavior was observed for **6HQNO** time-resolved fluorescence in methanol and water (Figure S8).[49] In pure methanol the fluorescence decay monitored at 380 nm consisted of a 100 ps component and a long-lived tail best approximated as a sum of 1.2 ns and 2.8 ns exponentials. As in the case of **MeHQNO** the amplitude of the tail directly depended on the age of the solution. The decay in MW measured at 380 nm was characterized by multiexponential decay with the lifetime of the short-lived dominating component around 27 ps. To summarize, because of photodecomposition only a limited amount of kinetic information on the *N*-oxides was reliable and reproducible. This included (1) the lifetimes of the fastest component measured at 380 nm in methanol and in MW; (2) the lifetimes of the asymptotic decays measured at 560 nm; and (3) single-exponential decays measured in the basic methanol and aqueous solutions.

The fluorescence decay of reference molecule **MeOQNO** in methanol was also nonsingle-exponential. The lifetime of the dominating (>96% amplitude) short-lived component was 0.6 ns in MeOH and 0.75 ns in MW.

## 4. Discussion

**4.1. Steady-State Spectra.** At neutral pH, we associate the 320 nm absorption of **6HQNO** with the neutral species, and at

(52) Janata, E. *Proc. Indian Acad. Sci. Chem. Sci.* **2002**, *114*, 731−737.

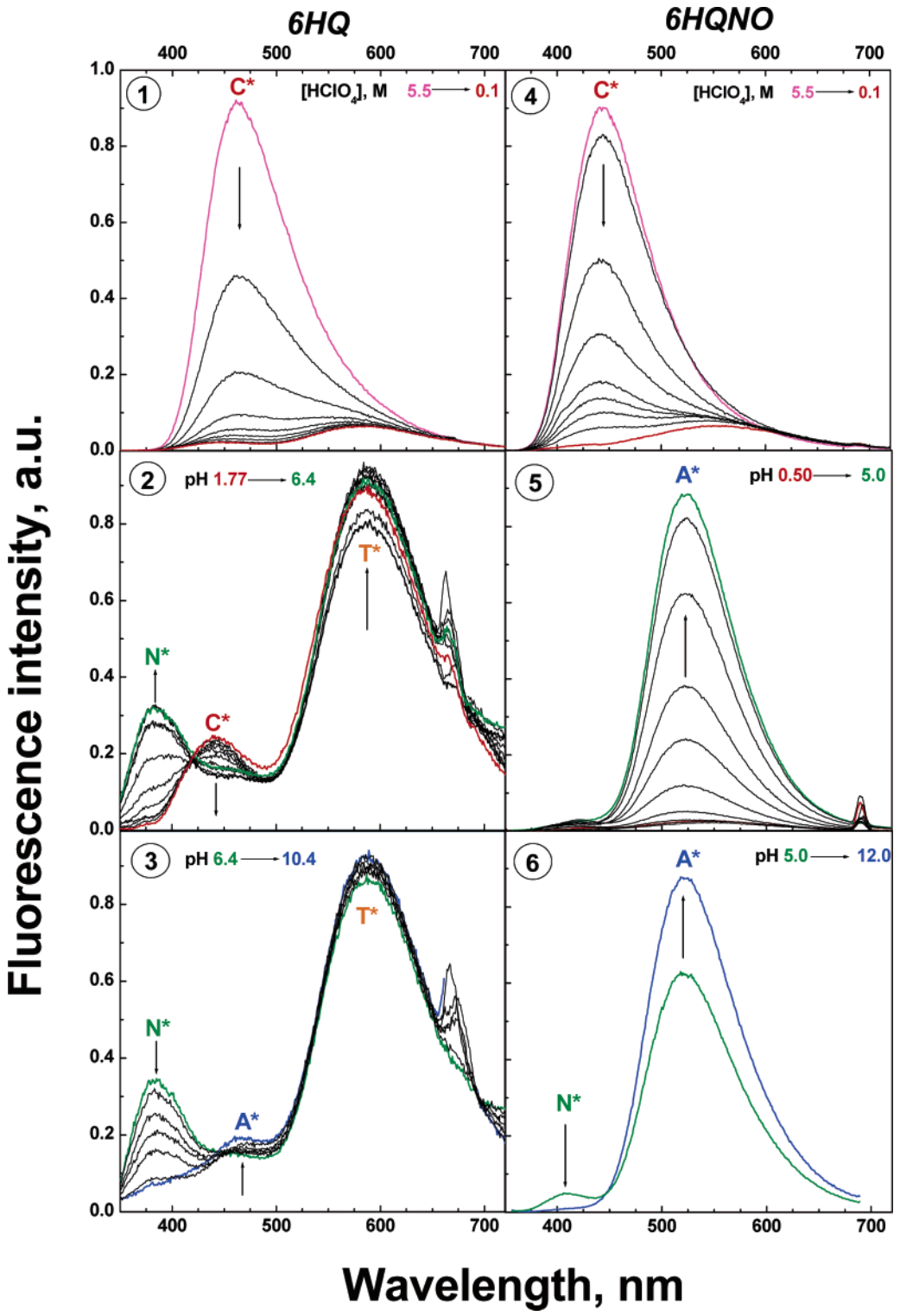


***Figure 7.*** Emission spectra of **6HQ** and **6HQNO** in 1/1 v/v water−methanol mixture as function of pH. (1) **6HQ** in extremely acidic pH region; (2) **6HQ** in acidic pH region; (3) 6HQ in basic pH region; (4) **6HQNO** in extremely acidic pH region; (5) **6HQNO** in acidic pH region; (6) **6HQNO** in basic pH region. In all cases the excitation wavelengths were long-wavelength isosbestic points for corresponding acid−base transitions. Emission bands of the excited neutral, cationic, anionic, and tautomer species are marked as N*, C*, A*, and T*, respectively.

high pH, the 385 nm absorption with the deprotonated anionic species. The equilibrium between neutral (ROH ≡ N) and *O*-deprotonated ($RO^-$ ≡ A) forms of **6HQNO**, characterized by a p$K_a$ of 8.01 (Figure 5) is about 1.2 p$K_a$ unit lower than that of parent **6HQ** in the same solvent.[1] It demonstrates a clear electron-withdrawing action of the N−O group. The low p$K_a$ value of the N−O group protonation, also observed in refs 39b and 53 for various quinoline *N*-oxides, demonstrates a decreased basicity as compared to heterocyclic hydrogen in **6HQ**. In the acidic media the *N*-oxides are known to be protonated by the

(53) Al-Zagoum, M. N.; Warren, G. G. *J. Inorg. Nucl. Chem.* **1969**, *31*, 3465−3470.

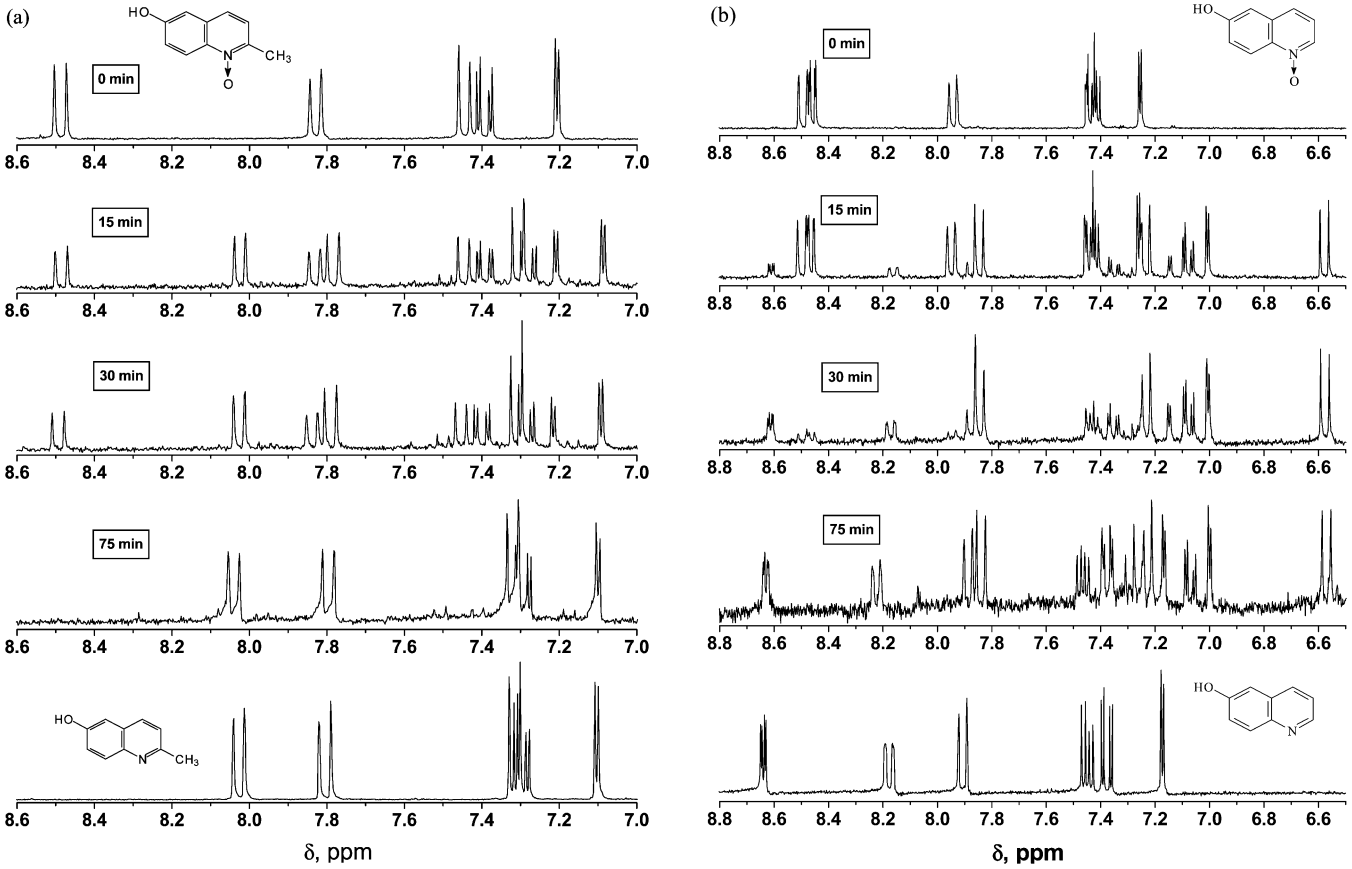


***Figure 8.*** $^1$H NMR spectra of (a) **MeHQNO** and (b) **6HQNO** in $CD_3OD$ during irradiation with 450 W Hanovia lamp as a function of time. Bottom spectra in each graph belong to the parent hydroxyquinoline. For MeHQNO only the aromatic region is shown.

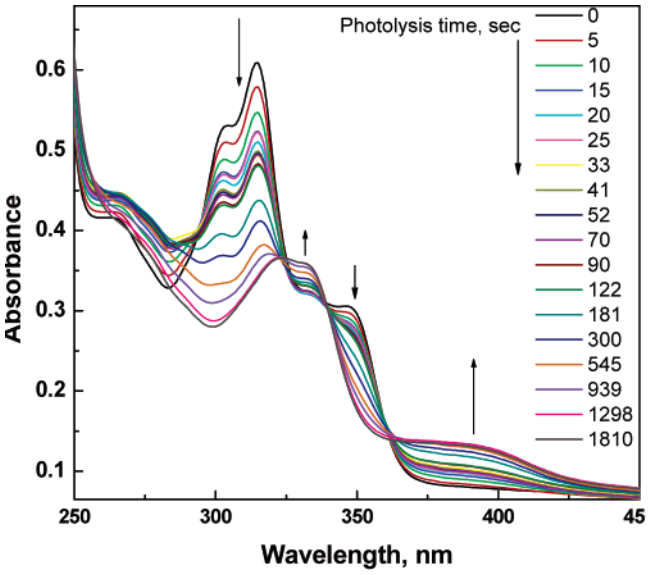


***Figure 9.*** UV spectra of **MeHQNO** in MW during the photolysis with 337 nm light.

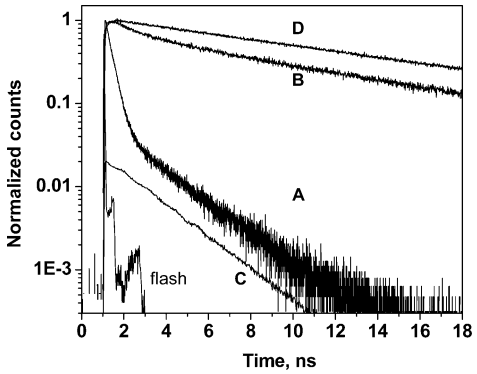


***Figure 10.*** Time-resolved fluorescence emission of **MeHQNO** and **MeHQ** in methanol. Kinetic traces correspond to: (A) decay of **MeHQNO** monitored at 380 nm; (B) decay of **MeHQNO** monitored at 560 nm; (C) decay of **MeHQ** monitored at 380 nm; (D) decay of **MeHQNO** in 0.01 M NaOH methanol solution monitored at 560 nm; IRF is also presented.

oxygen atom of the N−O group.[28] It is interesting to note that the absorption spectrum of **6HQNOH**$^+$ is essentially identical to those of **6HQH**$^+$ and *N*-methyl 6-hydroxyquinoline.[25a] Thus, we assume that the electronic structure of **6HQ** cation is insensitive to the chemical structure of the quarternizing group, H, OH, or methyl. Depending on pH, three ground-state species can exist: an N−O-protonated cation, neutral molecule, and *O*-deprotonated phenolate (Figure 5). Thus, the ground-state behavior of *N*-oxides resembles that of parent hydroxyquinolines, with modifications due to the relative p$K_a$'s. The reason for poor ground-state basicity and increased ground-state acidity of *N*-oxides is the electronic structure of the molecule, namely, the electron-withdrawing nature of the oxidized nitrogen atom.

The appearance of the low-energy emission band at 520−530 nm for *N*-oxides in neat methanol solution indicates an efficient ESPT process and a significant excited-state acidity. The large fluorescence quantum yield in methanol−water mixtures and the similarity of the emission maxima at neutral and basic (pH 12) solutions is evidence for the excited anion (R*O$^-$) formation, in contrast to hydroxyquinolines, for which

a double excited-state proton transfer leads to a tautomer as the dominant species (Figures 7 and S2).[49] In the latter case, upon further addition of NaOH up to 5 M concentration the emission of hydroxyquinolines is shifted to shorter wavelength, i.e., from a tautomer to purely anionic emission (see data for **MeHQ** at graph at Figure S2),[49] while the emission maxima and intensity of *N*-oxides remain the same. We conclude that the excited-state prototropic behavior of *N*-oxides in neutral and basic solutions is less complex than for hydroxyquinolines and does not involve the aromatic quinolinium nitrogen moiety as a strong photobase in the excited state, but only deprotonation of the hydroxyl group. Therefore, the spectral behavior of *N*-oxides in methanol and methanol−water mixtures as shown in Figures 6, 7, and S2[49] can be attributed to the well-known increase of the protolytic photodissociation rate with increasing water concentration.[54] In contrast, hydroxyquinolines show no ESPT in dry methanol, but in water in very wide pH range from 0 to 12 they demonstrate very weak fluorescence from the tautomer (zwitterion) formed as the result of double proton-transfer coupled to intramolecular charge transfer (Figure 7 and S2).[49]

In the acidic regime the prototropic behavior of *N*-oxides also differs from that of hydroxyquinolines and is even more intriguing. Let us analyze the possible reasons for the observed acid−base dependence of the fluorescence spectra of *N*-oxides.

The protolytic dissociation rate of *N*-oxides in MW is faster than $2.5 \times 10^{10}$ $s^{-1}$. From the known correlation between dissociation rate and equilibrium constant of various photoacids[55] one can estimate that p$K_a$* of *N*-oxides should be less than zero. Therefore the observed transition with apparent p$K_a$* around 2.6 (**6HQNO**) and 2.9 (**MeHQNO**) in MW is not the result of R*OH ↔ R*O$^-$ + H$^+$ equilibrium. On the other hand, this equilibrium is about 1.3 p$K_a$ unit higher than the ground-state *N*-protonation (Figure 5), so static quenching could also be ruled out.

As was mentioned earlier, quinoline-*N*-oxide and its various 4-substituted derivatives become *less* strong bases in the excited state;[39] thus, as a first guess it is natural to assume that *N*-oxides studied in the current work would have similar excited-state acid−base behavior. Note, however, that *N*-oxides studied in this work possess one of the strongest known electron-donor substituents (O$^-$);[56] therefore, we may assume that a minor increase in basicity upon excitation is not unreasonable. Thus, we may speculate that the weak emission at 560−580 nm in the acidic solutions of *N*-oxides (graph 5 at Figure 7 and graph 3 at Figure S2)[49] comes from the zwitterion (or tautomer) formed as a result of a secondary excited-state protonation of the *N*-oxide anion. Finally, we note that the adiabatic excited-state acid−base behavior of *N*-oxides is similar to that of 10-camptothecin (**10-CPT**), analyzed in the previous publication.[1] In the latter case, the chromophore-bearing **6HQ** unit had electronic-withdrawing substituents at 2 and 3 positions. As a result, the basicity of heterocyclic nitrogen was reduced, and no excited-state tautomerization was observed in neutral and acidic media. As in the case of *N*-oxides, the p$K_a$ of nitrogen protonation in **10-CPT** increased only by 1 unit upon excitation. As was mentioned earlier, the increased emission from the **6HQ** cation in the very acidic solutions is caused not by the shift of excited-state C*−T* equilibrium, but by the decreased activity of water acting as proton acceptor. In the solutions of the same the emission of cationic species of *N*-oxides becomes pronounced (graph 4 at Figure 7 and graph 3 at Figure S2)[49] probably because of the same effect of the decreasing water activity.

***Scheme 1***

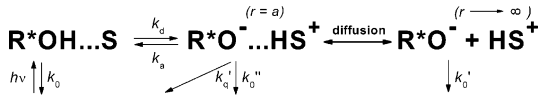


**4.2. Irreversible Photochemical Transformation of *N*-Oxides.** A detailed investigation of the photolysis mechanism was not the primary goal of the current research, and in a sense deoxygenation and rearrangement could be considered as parasitic parallel reactions that masks adiabatic proton transfer. We will not analyze in detail the mechanism of irreversible photolysis of *N*-oxides but will mention the main factors governing their reactivity. As was mentioned before, the photochemistry of hydroxyquinoline *N*-oxides has not been studied. However, the products of irreversible photolysis observed in this paper are not unique. 6-Methoxycarbostyril and 6-methoxyquinoline were the products of 6-methoxyquinoline-*N*-oxide (**MeOQNO**) photolysis in methanol.[29a] A prolonged irradiation of **MeOQNO** in methanol resulted in a photodimer not observed in our study.[29a] It is interesting that blocking the 2-position did not prevent 1−2 oxygen migration with rearrangement and a variety of photoproducts in the photolysis of 2-methylquinoline *N*-oxide in methanol.[29a] Surprisingly, the photolysis of **MeHQNO** in our work was very clean, leading to the parent **MeHQ** as the only photoproduct. The quantum yields of the photolysis did not depend on 2-methylation of **6HQNO** and the solvent. However, it was 2 times higher for **MeOQNO**, which is not capable of ESPT. Protolytic photodissociation of **6HQNO** and **MeHQNO** adds another deactivation channel for excitation that possibly competes with deoxygenation. Our experimental observations support the hypothesis that the deoxygenation mechanism may involve hydrogen atom abstraction from solvent as a first step.[57] The triplet state seems not to be involved here since the reaction occurs quite efficiently in air. It is interesting to speculate whether hydroxyl radicals[58] are formed during the photolysis.

**4.3. Time-Resolved Emission Data.** On the basis of these conclusions, we could have applied the usual two-step[54] kinetic scheme (Scheme 1) for ESPT reactions of hydroxyaromatic compounds for the analysis of the excited-state behavior of the *N*-oxides. This scheme was developed and used in the experimental and theoretical studies of reversible ESPT processes in solutions.[3,54,59]

Here we give only briefly the details of this approach. The first step involves protolytic dissociation to form a solvent−ion pair R*OH···S with intrinsic rate constant $k_d$. The solvent−ion pair can undergo both adiabatic and nonadiabatic (proton quenching) recombination with rate constants $k_a$ and $k_q$, respectively. The reversible reaction within the contact ion-

(54) Solntsev, K. M.; Huppert, D.; Agmon, N.; Tolbert, L. M. *J. Phys. Chem. A* **2000**, *104*, 4658−4669.
(55) See for example Figure 10 in: Solntsev, K. M.; Al-Ainain, S. A.; Il'ichev, Y. V.; Kuzmin, M. G. *J. Phys. Chem. A* **2004**, *108*, 8212−8222.
(56) Hansch, C.; Leo, A.; Taft, R. W. *Chem. Rev.* **1991**, *91*, 165−195.
(57) (a) Albini, A.; Fasani, E.; Frattini, V. *J. Photochem.* **1987**, *37*, 355−361. (b) Bucher, G.; Scaiano, J. C. *J. Phys. Chem.* **1994**, *98*, 12471−12473.
(58) Botchway, S. W.; Chakrabarti, S.; Makrigior, G. M. *Photochem. Photobiol.* **1998**, *67*, 635−640.
(59) (a) Pines, E.; Huppert, D.; Agmon, N. *J. Chem. Phys.* **1988**, *88*, 5620−5630. (b) Agmon, N.; Pines, E.; Huppert, D. *J. Chem. Phys.* **1988**, *89*, 5631−5638.

pair is followed by a diffusion second step in which the hydrated proton is removed from the parent molecule. The diffusion separation of proton and the excited anion is described by the Debye−Smoluchowski equation (DSE) with the characteristic constants $D = D_{H+} + D_{R*O-}$, the mutual diffusion coefficients of the proton and the conjugated base, and $R_D \equiv |z_1 z_2| e^2/k_B T\epsilon$, the Debye radius. The latter defines the Coulombic attraction potential $V(r) = -R_D/r$. The overall reaction involves electronically excited species, so one should consider the fluorescence lifetimes: $1/k_0 = \tau_0$ for the acid, $1/k_0' = \tau_0'$ for the base, and $1/k_0'' = \tau_0''$ for the contact ion pair. Usually, $\tau_0''$ is much longer than that for all other chemical and diffusion processes and can be ignored. A more detailed description of Scheme 1 and the method for kinetic parameters determination is given in the series of our preceding publications. Recently it was suggested to include a "loose" hydrogen-bonded complex into Scheme 1, therefore making ESPT a three-step process.[60]

Adiabatic and nonadiabatic geminate recombination of the excited R*O$^-$ and proton lead to nonexponential asymptotic behavior both in R*OH and R*O$^-$ time-resolved signals.[61] Thus, a full-value utilization of this scheme is possible only in the case of reliable nonexponential sets of kinetic data that are usually fitted to the numerical solutions of the time-dependent Debye−Smoluchowski equation (DSE).[62] As was mentioned previously, the photodecomposition is practically unavoidable in the case of *N*-oxides and the accumulation of the long-lived fluorescent photoproduct masks long-time nonexponential asymptotic behavior of *N*-oxides fluorescence. As a result, a determination of $k_a$ and $k_q$ from the kinetics data becomes impossible, although we can associate the fastest exponential component in the R*OH decay with the lifetime-corrected steady-state rate of proton transfer, $k_d^{ss}$.

The reason for this is the following. In accordance with recent investigations of the diffusion-controlled geminate reactions,[63] the most prominent kinetic regime for R*OH decay is the Smoluchowski one even in the geminate case,

$$[\mathrm{R^*OH}](t) \approx \exp(-K_{eq}^{-1}\int_0^t k(t')\mathrm{d}t'), \tag{1}$$

where the concentration is substituted by the reciprocal equilibration constant, $K_{eq} = \kappa_a/k_d$,

$$k(t) = \kappa_a \frac{k_D + \kappa_a \exp(x)\mathrm{erfc}\sqrt{x}}{k_D + \kappa_a} \tag{2}$$

$$x = (1 + \kappa_a/k_D)^2 Dt/R^2$$

$$\kappa_a = 4\pi R^2 k_a \exp(-V(R)) \tag{3}$$

$$k_D = 4\pi D R_{eff} \tag{4}$$

$$R_{eff} = R_D/(1 - \exp(-R_D/R))$$

where $\kappa_a$ is the recombination rate constant, $k_D$ is the diffusion rate constant, $R_D$ is the Debye radius and $R$ is the radius of the contact ion pair.

In the beginning the decay rate of the reactive species, $K_{eq}^{-1}k(0)$, is the intrinsic reaction rate, $k_d$, which then switches to its steady-state value,

$$k_d^{ss} = \frac{k_d}{1 + \kappa_a/k_D} \tag{5}$$

The characteristic time of this switch, $t_{sw}$, corresponds to the point where $x \approx 1$,[64,65] i.e.

$$t_{sw} \approx \frac{R^2/D}{(1 + \kappa_a/k_D)^2}. \tag{6}$$

Using kinetic and diffusion values for similar system 5-cyano-2-naphthol in methanol−water mixtures[54] ($k_a \approx 23$ Å/ns, $D \approx 4.07 \times 10^{-5}$ cm$^2$/s, $R_D \approx 9.57$ Å, $R \approx 5.5$ Å for MW, and $k_a \approx 16$ Å/ns, $D \approx 3.66 \times 10^{-5}$ cm$^2$/s, $R_D \approx 17.2$ Å, $R \approx 5.5$ Å for MeOH) one obtains $t_{sw} \approx 20$ ps for MW and 10 ps for MeOH. It means that the steady-state regime is reached very rapidly and could not be detected with the present picosecond time-resolved apparatus. However, $k_d$ is larger than $k_d^{ss}$ only by the factor of 1.5−2.

Thus, in this case

$$k_d^{ss} = 1/\tau_1 - 1/\tau_0 \tag{7}$$

where $\tau_1$ is the lifetime of the shortest exponent in the multiexponential fit of R*OH signal and $\tau_0$ is the lifetime of *N*-oxides in the absence of ESPT assumed to be equal to that of **MeOQNO**. Note that $\tau_0$ sums all non-ESPT deactivation processes including photodeoxygenation, which competes with the adiabatic protolytic dissociation. The dissociation rate constant of **6HQNO** in methanol (8.3 1/ns) was close to that of the fastest known photoacid, 5,8-dicyano-2-naphthol,[66] and was 2 times larger than Debye relaxation time of MeOH at room temperature.

It is impossible to determine excited-state acidity constant p$K_a$* from the kinetic measurements since reliable determination of $k_a$ values is complicated by irreversible photodecomposition. Another approach for p$K_a$* determination is the Förster equation

$$\mathrm{p}K_a - \mathrm{p}K_a^* = 2.097 \times 10^4 (1/\lambda_{abs} - 1/\lambda'_{abs}) \tag{8}$$

where $\lambda_{abs}$ and $\lambda'_{abs}$ are absorbance maxima of ROH and RO$^-$, respectively. However, a complicated nature of ROH absorption, namely the overlap of several transition bands without distinct low-energy maximum makes the validity of Förster approach questionable. Nevertheless, it is interesting to note that usage of *major* low-energy ROH absorption maxima of *N*-oxides in the Förster equation gave p$K_a$* values around −3, which places excited-state acidity of the hydroxyaromatic *N*-oxides between dicyano- and monocyano 2-naphthols.[3] This is in excellent agreement with our time-resolved data.

A list of spectral and kinetic characteristics and p$K_a$* of *N*-oxides are given in Table 2.

(60) Rini, M.; Pines, D.; Magnes, B.-Z.; Pines, E.; Nibbering, E. T. J. *J. Chem. Phys.* **2004**, *121*, 9593−9610.
(61) (a) Gopich, I. V.; Solntsev, K. M.; Agmon, N. *J. Chem. Phys.* **1999**, *110*, 2164−2174. (b) Agmon, N. *J. Chem. Phys.* **1999**, *110*, 2175−2180. (c) Solntsev, K. M.; Agmon, N. *Chem. Phys. Lett.* **2000**, *320*, 262−268.
(62) Krissinel, E. B.; Agmon, N. *J. Comput. Chem.* **1996**, *17*, 1085−1098.
(63) (a) Popov, A. V.; Agmon, N. *Pol. J. Chem.* **2003**, *77*, 1659−1668. (b) Agmon, N.; Popov, A. V. *J. Chem. Phys.* **2003**, *119*, 6680−6690.
(64) Gladkikh, V. S.; Burshtein, A. I.; Tavernier, H. L.; Fayer, M. D. *J. Phys. Chem. A* **2002**, *106*, 6982−6990.
(65) Popov, A. V.; Agmon, N. *J. Chem. Phys.* **2002**, *117*, 4376−4385.
(66) Cohen, B.; Huppert, D. *J. Phys. Chem. A* **2001**, *105*, 2980−2988.

***Table 2.*** Spectral and Kinetic Parameters of *N*-Oxides

| | compound | | | |
|---|---|---|---|---|
| | 6HQNO | | MeHQNO | |
| | solvent | | | |
| parameter | MeOH | MW | MeOH | MW |
| ROH $\lambda_{max}^{abs}$, nm[a] | 323 | 319 | 317 | 315 |
| $RO^-$ $\lambda_{max}^{abs}$, nm | 389 | 385 | 374 | 382 |
| R*OH $\lambda_{max}^{fluor}$, nm | 407 | 407 | 386 | 400[b] |
| $R^*O^-$ $\lambda_{max}^{fluor}$, nm | 532 | 521 | 516 | 508 |
| $k_d^{ss}$, 1/ns | 8.3 | 36 | 2.3 | 26 |
| $\tau_0'$, ns | 9.9 | 10.4 | 12.0 | 12.0 |
| $\tau'$, ns | 9.0 | 10.3 | 10.0 | 12.0 |
| p$K_a$* (Förster) | | −3.2 | | −2.9 |

[a] Major low-energy absorbance peak. [b] Large experimental error.

An overall kinetic scheme of ESPT in the systems investigated and the summary of photolysis experiments are presented in Figures S9 and S10, respectively.

## 5. Conclusions

As we have demonstrated previously, the acidity of hydroxyarenes shows a unique dependence on the structure of the photoacid. Hydroxyquinoline *N*-oxides join the class of photoacids with remarkable excited-state acidity, combining the kinetic efficiency of a hydroxyquinoline without its energy-wasting tautomerization. The combination of enhanced ESPT reactivity and efficient photodeoxygenation in tandem with bright fluorescence makes these compounds possible candidates for the modulation of biological activity with simultaneous monitoring by fluorescence spectroscopy/microscopy methods. However, the biological consequences of the accompanying side reaction may provide an additional complication to such studies. Other substitution patterns may provide alternative which minimize such complications.

**Acknowledgment.** Support of this research by the U.S. National Science Foundation (Grant CHE-0096941) and the U.S.-Israel Binational Science Foundation is gratefully acknowledged. National Science Foundation Grant BIR-9306392 is acknowledged for partial funding of the solution NMR spectrometers. We thank Drs. Janusz Kowalik for the help with the characterization of new compounds and Alexander Popov for valuable discussion.

**Supporting Information Available:** More spectral data on absorption and emission properties of *N*-oxides; photolysis of various compounds monitored by NMR; fluorescence kinetic curves; overall ESPT kinetic scheme and photolysis summary. This material is available free of charge via the Internet at http://pubs.acs.org.

JA0514545